



Hydrophilic Crosslinked TEMPO-Methacrylate Copolymers – a Straight Forward Approach towards Aqueous Semi-Organic Batteries

Lada Elbinger^{+, [a, b]} Erik Schröter^{+, [a, b]} Christian Friebe^{+, [a, b]} Martin D. Hager^{+, [a, b]} and Ulrich S. Schubert^{*, [a, b]}

Crosslinked hydrophilic poly(2,2,6,6-tetramethylpiperidiny-N-oxyl-co-[2-(methacryloyloxy)-ethyl]trimethyl ammonium chloride) [poly(TEMPO-co-METAC)] polymers with different monomer ratios are synthesized and characterized regarding a utilization as electrode material in organic batteries. These polymers can be synthesized rapidly utilizing commercial starting materials and reveal an increased hydrophilicity

compared to the state-of-the-art poly(2,2,6,6-tetramethylpiperidiny-N-oxyl-4-methacrylate) (PTMA). By increasing the hydrophilicity of the polymer, a preparation of cathode composites is enabled, which can be used for aqueous semi-organic batteries. Detailed battery testing confirms that the additional METAC groups do not impair the battery behavior while enabling straight-forward zinc-TEMPO batteries.

Introduction

For many years, lithium-ion batteries (LIBs) have been among the most favorable technologies at the market of energy storage devices. The LIB is one of the most advanced electrochemical storage technologies and demonstrates high energy densities and extremely high cyclabilities.^[1] However, the global energy demand is rising and cannot be met relying on lithium-based technologies alone, leading to the development of alternative battery cell chemistries over the last years. Among them, active materials based on organic compounds are promising as they allow for tailor-made active materials and renewable synthesis routes. This offers different processing possibilities, which are not conceivable with most metal batteries, for instance screen or ink-jet printing.^[2] Furthermore, other casting methods or roll-to-roll processing techniques are imaginable, which facilitates the production of mechanically flexible batteries, as can be desired for “internet of things” application scenarios.^[3]


The typically required electrolytes for the traditional LIBs are of organic nature. The wide electrochemical stability window of organic electrolytes makes them favorable for lithium batteries and, consequently, high cell voltages can be achieved. However, organic electrolytes show a rather low conductivity and are expensive, often toxic and volatile. Moreover, common lithium-based technologies are sensitive to physical stress, which can lead to battery failure, leakage, or, ultimately, hazardous degeneration reactions. Despite the narrower potential stability window of aqueous solutions, water-based electrolytes are considered as a promising alternative as they are non-toxic, cost-efficient, and rapidly processable. Therefore, batteries utilizing aqueous electrolytes are expected to be a promising alternative for batteries of the current LIB generation.^[4] However, the thermodynamic stability window of water is limited to 1.23 V, beyond which harmful hydrogen and oxygen evolution reactions (HER/OER) occur. It is possible to extend the stability window of water, for which several systems with highly concentrated salt electrolytes were investigated recently.^[5] Challenges of this method are high costs and a tendency towards salt crystallization during long-term cycling in the battery, which can lead to a complete failure of the battery.^[6] Another method is the use of matching electrodes. Suitable for aqueous coin cell batteries can be zinc electrodes, which are of low cost, low toxicity and exhibit high stability in aqueous solutions.^[7] In addition, aqueous zinc batteries show high energy density, which derives from the high specific capacity of the metallic zinc electrode.^[4]


During recent years, many different organic active materials whose electrochemical properties are compatible with those of metallic zinc anodes have been researched and tested for rechargeable zinc batteries.^[8] The general mechanisms of redox reactions differ from material to material and, thus, the cathodes have been classified into three types, namely p, n and bipolar.^[9] The charged state of a p-type material is its oxidized state, when it transforms from a neutral state (p) to the

[a] L. Elbinger,⁺ E. Schröter,⁺ Dr. C. Friebe, Dr. M. D. Hager, Prof. Dr. U. S. Schubert
Laboratory of Organic and Macromolecular Chemistry (IOMC)
Friedrich Schiller University
Humboldtstraße 10, 07743 Jena (Germany)
E-mail: ulrich.schubert@uni-jena.de

[b] L. Elbinger,⁺ E. Schröter,⁺ Dr. C. Friebe, Dr. M. D. Hager, Prof. Dr. U. S. Schubert
Center for Energy and Environmental Chemistry (CEEC)
Friedrich Schiller University
Philosophenweg 7a, 07743 Jena (Germany)

[†] These authors contributed equally to this work.

 Supporting information for this article is available on the WWW under <https://doi.org/10.1002/cssc.202200830>

 © 2022 The Authors. ChemSusChem published by Wiley-VCH GmbH. This is an open access article under the terms of the Creative Commons Attribution Non-Commercial License, which permits use, distribution and reproduction in any medium, provided the original work is properly cited and is not used for commercial purposes.

positively charged (p+). Representative examples of such materials are polyindole, 2,2,6,6-tetramethylpiperidiny-*N*-oxyl (TEMPO) and poly(vinyl-2-[9-(1,3-dithiol-2-ylidene)anthracen-10(9H)-ylidene]-1,3-dithiole) (exTTF).^[10] n-Type materials are charged through reduction and thereby transform from a neutral state (n) into a negatively charged (n-) one. The most common examples for n-type materials are different quinones and pyrene-4,5,9,10-tetraone (PTO).^[11] The bipolar type is capable of performing both processes and can be transformed from a neutral state (b) to a positive (b+) or negative state (b-), for example, the conductive polymer poly(p-phenylene) (PPP).

One of the most thoroughly investigated organic p-type structures that show high potential for application in batteries is TEMPO, which bears a redox active and sterically protected nitroxyl radical (Scheme 1). TEMPO has been used as a redox-active moiety in numerous application scenarios, such as sensors and catalysts.^[12] The nitroxyl radical molecule undergoes reversible one-electron redox reactions in both organic and aqueous electrolytes, exhibiting high redox potentials and fast reaction kinetics.^[13] Batteries with TEMPO-based polymer cathodes are well-known and exhibit outstanding cyclabilities, high energy densities and cell voltages, compared to the other known organic cathode materials.^[14]

Until now, poly(2,2,6,6-tetramethylpiperidiny-*N*-oxyl-4-methacrylate) (PTMA) polymers have been most commonly used as organic TEMPO-bearing active materials for cathodes. However, PTMA polymers show a low polarity and are therefore rather hydrophobic. Thus, they are not suitable for the combination with aqueous electrolytes. However, aqueous electrolytes are of particular interest because they show a high conductivity, which can be one order of magnitude higher compared to organic electrolytes.^[15]

To change the polarity and introduce hydrophilicity to the cathode material, theoretically, there are two strategies. The first possibility represents changing the basic structure of the polymer. Koshika *et al.* introduced poly(2,2,6,6-tetramethylpiperidiny-*N*-oxyl-4-vinyl ether) (PTVE) as new battery material, which is compatible with aqueous electrolytes, as was shown for more than 500 cycles.^[16] However, the synthesis of the TEMPO vinyl ether monomer and the polymerization process are time-consuming and expensive due to the necessary iridium catalyst for the coupling and the cooling during the polymerization step.^[17]

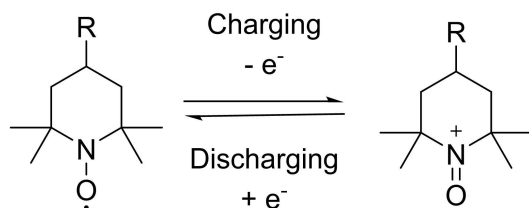
Another way to obtain a polymer with an increased hydrophilicity is the incorporation of a hydrophilic comonomer that mediates the desired properties into the polymer chain. There

are several monomers that are suitable for this purpose. Hagemann *et al.* successfully synthesized a TEMPO-containing zwitterionic polymer with [(2-(methacryloxy)ethyl)dimethyl-(3-sulfopropyl)]ammonium hydroxide as a solubilizing comonomer and investigated the polymer as a catholyte for aqueous redox flow batteries.^[18] Hatakeyama-Sato *et al.* worked with hydrophilic poly(2,2,6,6-tetramethylpiperidiny-*N*-oxyl-4-acrylamide) (PTAm) and further increased the hydrophilic properties of the polymer by applying hydrophilic acrylic acid.^[19] In this work, [2-(methacryloxy)ethyl]trimethyl ammonium chloride (METAC) is utilized as this comonomer has been successfully used for aqueous redox flow batteries before.^[20] By this new approach, hydrophilic crosslinked PTMA is used as cathode material for water-based organic batteries. To investigate the cathode performance, cells with an oversized zinc electrode and aqueous zinc bis(trifluoromethanesulfonyl)imide (ZnTFSI₂)- or zinc trifluoromethanesulfonate [Zn(OTf)₂]-containing electrolytes are applied.

Results and Discussion

With the targeted utilization of an aqueous electrolyte in a TEMPO-based polymer battery, we started with a straightforward approach to validate the hydrophobic nature of the standard PTMA composite and prepared coin cells with PTMA-containing composite electrodes [SuperP as conductive agent and poly(vinylidene difluoride) (PVDF) as binder]. The organic cathode material was combined with a zinc metal counter electrode and with aqueous electrolytes, namely, aqueous ZnTFSI₂ and Zn(OTf)₂. Zinc was chosen as it is known to act as a water-compatible, oversized electrode material with reversible redox chemistry. After application of the standard test protocol (see Experimental Section), it could be concluded that classical PTMA cathodes are not suitable for the aqueous electrolytes as no reversible charge/discharge behavior was observed. This observation can be explained by the hydrophobic nature of PTMA and the nonpolar additional components in the cathode, such as conductive additives, (*e.g.*, SuperP®), and the binder. Both components decrease the hydrophilicity of the resulting composite even further. As a result, the aqueous electrolyte is not able to penetrate the cathode and the redox processes cannot take place.

To significantly increase the hydrophilicity of the cathode materials, we performed a copolymeric approach, comprising the redox-active TEMPO-bearing monomers (TEMPO-methacrylate) from the PTMA active material and the solubility mediator METAC, which is known from the work on aqueous polymer-based redox flow batteries of the Schubert group.^[20] As described in the introduction, we have chosen the co-polymerization of 2,2,6,6-tetramethylpiperidiny-*N*-oxyl-methacrylate (TEMPMA) and METAC in different hydrophilicity mediator : monomer ratios. While hydrophilicity is required, water solubility must be strictly avoided. Furthermore, a higher METAC ratio also goes in hand with a lower theoretical specific capacity of the active material. Consequently, a crosslinker was applied,



Scheme 1. Schematic representation of the TEMPO-based redox processes upon charging/discharging.

namely poly(ethylene glycol diacrylate) (PEGDA) because of its intrinsic hydrophilicity.

A molar ratio of 2 mol% was chosen because higher amounts lead to overly strong crosslinking within the polymer matrix, which decreases the swellability of the active material. However, insufficient crosslinking should also be avoided since a weakly crosslinked polymer matrix can contain remaining soluble short polymer chains, which enable shuttle processes of TEMPO molecules/oligomers, leading to pronounced self-discharge of the battery. To investigate the influence of the hydrophilicity mediator on the performance of organic thin-layer batteries, it was decided to synthesize and evaluate different TEMPMA : METAC ratios namely 50:50, 80:20, 95:5 and 98:2. The crosslinked polymer networks were synthesized by free radical polymerization of TEMPMA, METAC and PEGDA with different molar ratios in aqueous HCl solution at 80 °C. The free radical polymerization was selected for this purpose because of its short reaction times and simple handling. Further, it is possible to utilize commercial starting materials, which enable simple upscaling possibilities. The prepared crosslinked polymers were lyophilized and finely ground. This step is a prerequisite for the next oxidation step as it provides a better penetrability for the oxidation agent and catalyst. Without good penetration, the non-accessible piperidine moieties are not oxidized, which decreases the degree of oxidation, ultimately leading to low capacities. Subsequently, the oxidation reaction was performed in a 50:50 ethanol/water mixture to improve the polymer swelling and support the oxidation, which directly affects the resultant degree of oxidation. Hydrogen peroxide was chosen as oxidative agent and the reaction is catalyzed with sodium tungstate, according to the procedures presented by Muench *et al.*^[21] After lyophilization, the solid polymers were analyzed *via* electron paramagnetic resonance (EPR) measurements for the determination of the degree of oxidation. As the obtained degrees of oxidation were not suitable (< 60% for all polymers), the materials were oxidized a second time following the same procedure with a higher amount of peroxide. This yielded sufficient degrees of oxidation for the 50:50 (70.1%), 80:20 (75.1%), 95:5 (73.2%) and 98:2 (75.0%) polymers. The values after the first oxidation reaction are presented in the Experimental Section (Table 4).

Thermogravimetric analysis (TGA) was performed to analyze the thermal stability of the polymers (Figure 1). The decomposition temperatures were determined at a mass loss of the measured polymer of 5%. The measured curves show some shoulders, which can be explained by the uncontrolled nature of the free radical polymerization. Domains with variable chain lengths can be formed, which potentially reveal a different decomposition behavior. The samples that contain higher mediator ratios lead to multiple shoulders in the TGA curves. The thermogravimetric curves of the polymers featuring monomer ratios of 95:5 and 98:2 are quite similar to each other, which can be explained by the very similar polymer composition. From the TGA, the decomposition temperatures for the four polymers were obtained at 185 °C (50:50), 227 °C (80:20), 246 °C (95:5), and 248 °C (98:2), showing that a higher amount of mediator results in a lower degradation temperature.

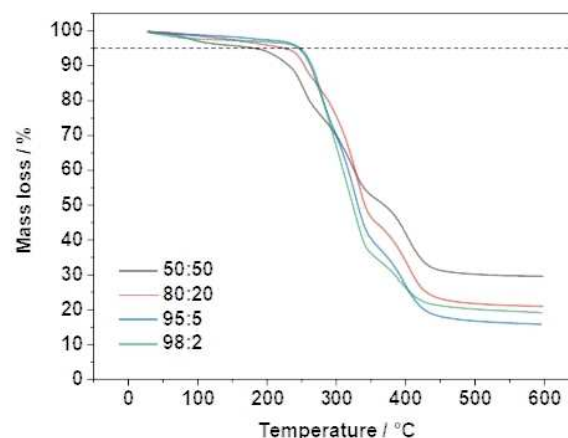


Figure 1. The thermogravimetric curves of the different polymers.

The stability of the polymers is also further confirmed by differential scanning calorimetric analysis. The corresponding information can be obtained from the Supporting Information (Figure S2).

In order to evaluate if the comonomer METAC leads to undesired side effects on the TEMPO-bearing polymer, electrochemical characterization of the copolymers was performed. For this purpose, coin cells based on the crosslinked poly(TEMPO-*co*-METAC) composite electrodes, featuring PVDF as binder and SuperP® as conductive agent were constructed and fabricated to 2032-type coin cells under ambient conditions with aqueous electrolytes. The cycling protocols were chosen similar to the investigations performed by Muench *et al.* in order to compare the new material to the well-established PTMA.^[21] For zinc batteries, many zinc salts as well as combinations of different salts are common.^[22] However, to reduce the complexity of the cell, we decided to focus on a single-salt electrolyte approach without further addition of dendrite-preventing additives. Triflate (OTf) and *bis*(trifluoromethanesulfonyl)imide (TFSI) zinc salts were utilized. Cyclic voltammetry (CV) potentials for the ZnTFSI₂- and Zn(OTf)₂-containing batteries are summarized in Table 1 and the obtained cyclic voltammograms at 0.1 mVs⁻¹ are depicted in Figure 2.

The CV curves exhibit reversible signals in the range between 1.4 V and 1.6 V (vs. Zn/Zn²⁺), which indicates that the

Table 1. Utilized ratios of TEMPO-METAC with achieved degrees of oxidation. Redox potentials of the zinc-polymer batteries. Values were obtained from the redox signals at 0.1 mVs⁻¹ scanning speed.

Feed ratio TEMPO: METAC	50:50	80:20	95:5	98:2
Degree of oxidation [%]	70 ± 3	75 ± 5	73 ± 5	75 ± 12
Potential [V] 2 M Zn(OTf) ₂ ^[a]	1.51	1.49	1.51	1.51
Potential [V] 2 M ZnTFSI ₂ ^[a]	1.42	1.42	1.43	1.47
Specific capacity [mAh g ⁻¹] ^[b]	55.5	88.8	105.5	108.8

[a] Potentials vs. Zn/Zn²⁺. [b] Specific capacities calculated from specific capacity of PTMA.

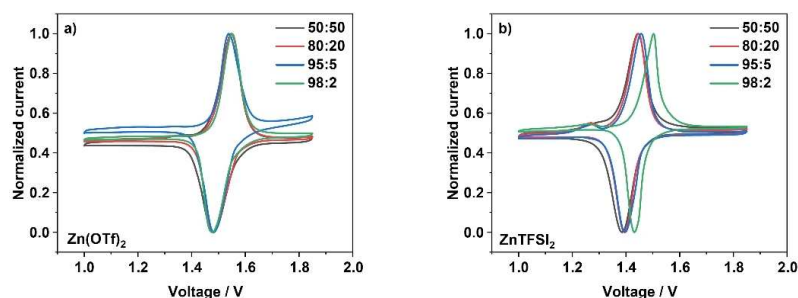


Figure 2. CV curves of the Zn/poly(TEMPO-co-METAC) batteries for (a) Zn(OTf)₂ electrolyte and (b) ZnTFSI₂ electrolyte at 0.1 mV s⁻¹ scanning speed. The active monomer/hydrophilicity mediator ratios are given in the graphs.

reversible redox behavior of the TEMPO-moieties is retained after copolymerization, and no disturbing influence of the METAC group is present. This is in accordance with similar materials, which have been utilized in aqueous polymer-based redox flow battery systems.^[23] Also, the peak shapes do not differ significantly, except for the 98:2-ratio ZnTFSI₂-containing batteries, which exhibit a slightly higher half-wave potential, which is referred to a lower wettability and the consequent overpotentials. The electrodes were then subjected to galvanostatic cycling at 1 C to provide information on the cyclability of the composite electrodes (Figure 3). Five cycles were obtained for each cell, which suggested reversible charging/discharging behavior.

The curves depict reversible battery cycles between 1.0 V and 1.7 V (vs. Zn/Zn²⁺) with stable charging/discharging plateaus at approximately 1.55 V for the Zn(OTf)₂ electrolyte and 1.45 V for the ZnTFSI₂. Coulombic efficiencies of 98% were obtained for five cycles. No signs of degradation caused by METAC are observed and the curves resemble quite accurately the expected shapes for an aqueous TEMPO-zinc-battery. From these initial investigations, detailed testing was performed to prove the feasibility of the hydrophilic crosslinked copolymers

in aqueous battery systems. Rate capability testing, self-discharge tests, long-term cycling, and float testing were executed, following a strategy applied by Muench *et al.* for the synthesized PTMA nanoparticles, which represent the ideal material for comparison.^[21] Charging rate tests have been performed for both ZnTFSI₂ (Figure 4) and Zn(OTf)₂ electrolyte (Figure 5).

The ZnTFSI₂-containing cells show PTMA-typical rate capability behavior, with the addressed capacity decreasing at increasing charging/discharging rates.^[21] Even though the ratio of hydrophilicity mediator varies, all batteries can be run at standard testing conditions and the TEMPO-moieties appear to be addressable. For all batteries, the charging capacity at 1 C can be re-obtained after cycling at higher C-rates. This indicates a reversible charge/discharge mechanism without significant degradation of the active material at higher charging currents. While standard PTMA shows a specific capacity of 111 mAh g⁻¹, the solubility mediator leads to a decreased specific capacity, depending on its content in the polymer. Consequently, the 50:50 mixture exhibits a specific capacity of 56 mAh g⁻¹ (Table 1). This value increases with increasing amounts of TEMPO-carrying monomer in the polymer to 89 mAh g⁻¹ for the

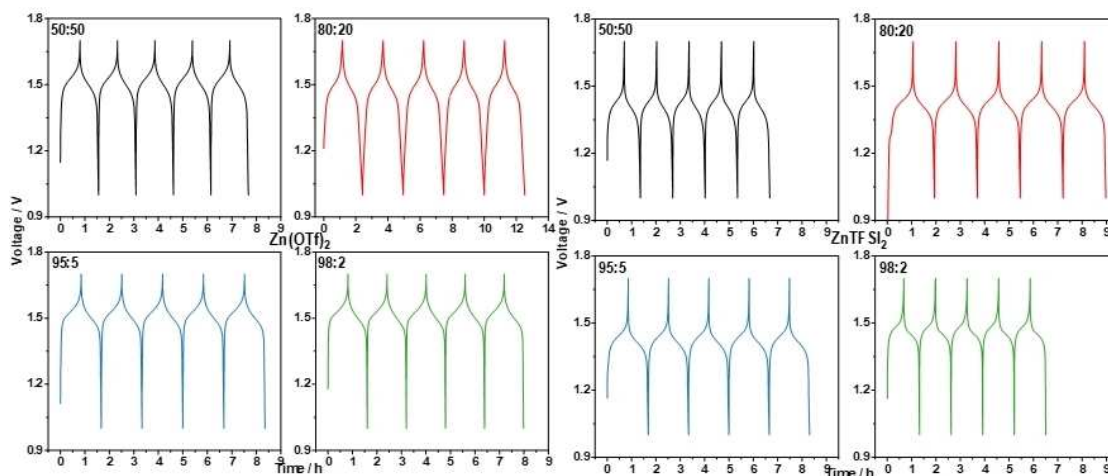


Figure 3. Voltage curves for the Zn(OTf)₂- (left) and ZnTFSI₂-containing (right) polymer-zinc batteries. Monomer ratios of 50:50 (black), 80:20 (red), 95:5 (blue) and 98:2 (green) were investigated and galvanostatically cycled at 1 C charging/discharging rate.

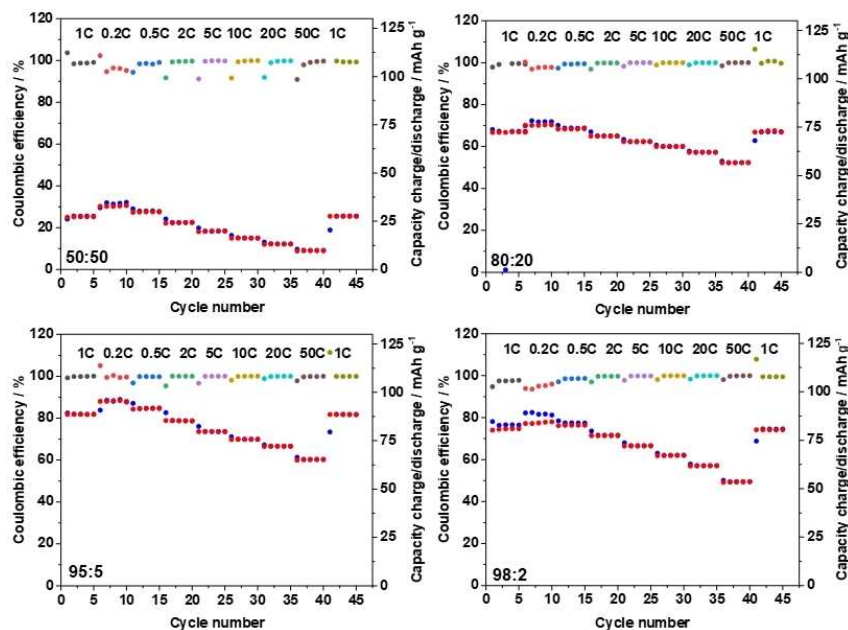


Figure 4. Summary of the rate capability tests that have been performed for the ZnTfSI₂ electrolyte-containing polymer-zinc batteries. C-rates of 1, 0.2, 0.5, 2, 5, 10, 20, and 50 C were applied.

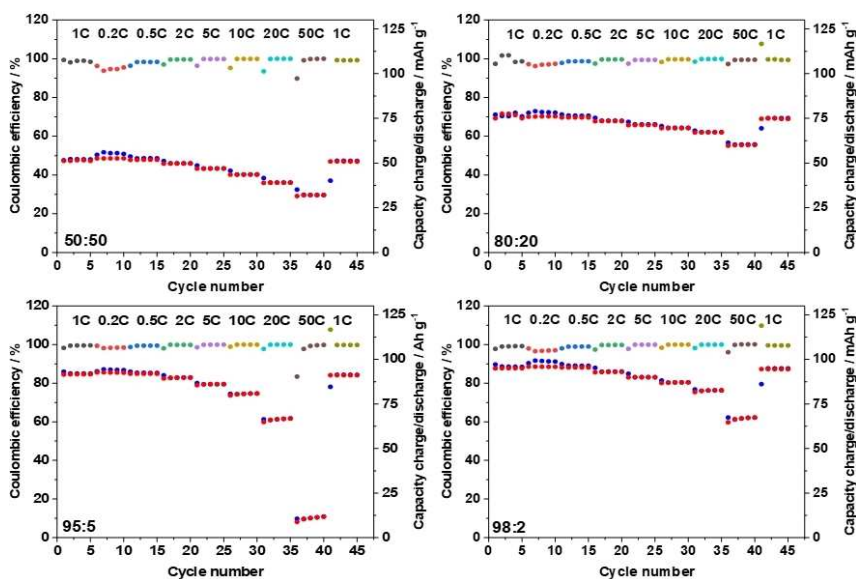


Figure 5. Summary of the rate capability tests that have been performed for the Zn(OTf)₂ electrolyte-containing polymer-zinc batteries. C-rates of 1, 0.2, 0.5, 2, 5, 10, 20, and 50 C were applied.

80:20 ratio, 106 mAh g⁻¹ for the 95:5 ratio and 109 mAh g⁻¹ for the 98:2 ratio. This trend can also be observed by comparing the rate testing diagrams for the different polymer ratios. However, the theoretical values (108.8 mAh g⁻¹ for 98:2, 105.5 mAh g⁻¹ for 95:5, 88.8 mAh g⁻¹ for 80:2, 55.5 mAh g⁻¹ for 50:50) are not obtained for any of the mixtures.

The identical rate testing experiments were also performed for the Zn(OTf)₂ electrolyte. However, for the polymer ratios with the lowest polarity (98:2 and 95:5), the batteries were

subjected to five cycles of floating, prior to the rate testing experiments. This procedure was necessary as a pronounced wetting process, with a successive capacity increase over all charging rates was observed when cells were directly used in rate testing experiments.

Thus, at lower mediator ratios, the behavior of the material drifts towards the non-polar PTMA. However, already very low amounts of mediator make the TEMPO-groups more addressable for aqueous electrolytes, if the system is actively precondi-

tioned with a suitable technique, which keeps the material in charged state for an extended period of time.

In total, the addressed capacities are higher than those for the ZnTFSI₂ electrolytes, resulting in charge capacities that are closer to the theoretical specific capacity of the respective polymers. A summarized overview of the addressable capacities of the batteries at different C-rates is given in Figure 6.

When higher amounts of mediator are used, the expected rate-capability behavior is obtained also for the Zn(OTf)₂ electrolyte without any signs of wetting processes. At a ratio of 80:20, a capacity retention of approximately 80% is measured for the highest charging rate. The capacity retention for the 50:50 ratio is significantly lower at around 65% at 50 C. Interestingly, the 95:5 ratio shows an extremely low capacity retention around 10%, which differs significantly from the approximately 60% of the 98:2 ratio. With the ZnTFSI₂-based electrolyte, 72% capacity retention are obtained for the 80:20 ratio at 50 C. With lower mediator amounts, the capacity retention is slightly decreased to 68% for the 95:5 ratio and to 64% for the 98:2 ratio. The 50:50 ratio exhibits a lower capacity retention: only 60% of the reference capacity are obtained already at a rate of 5 C and it decreases even to 30% at 50 C. Overall, the performance of the ZnTFSI₂ cells can be considered excellent and is certainly an improvement compared to previous systems. The results of the rate capability tests match the diagrams for the material usage, which is shown in Figure 7. Overall, high material usages are observed for the lower charging rates of 0.2 to 2 C, varying between 95 and 80%. However, as observed for the capacity retention, the ZnTFSI₂-containing batteries reveal significantly lower material utiliza-

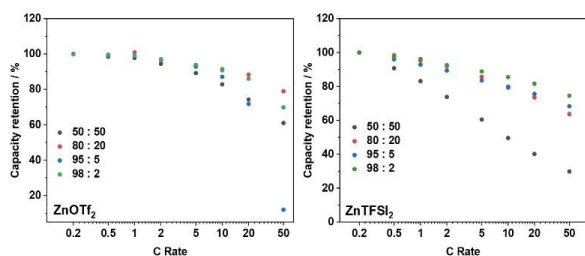


Figure 6. Capacity retention during rate capability testing for Zn(OTf)₂- (left) and ZnTFSI₂-based (right) electrolyte. Normalized to discharge capacity that was achieved for a current of 0.2 C.

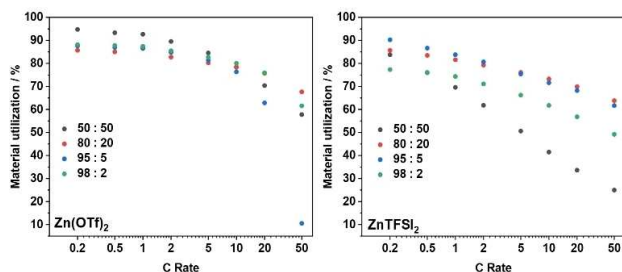


Figure 7. Material utilizations for the Zn(OTf)₂ (left) and the ZnTFSI₂ (right) batteries. 100% Material utilization corresponds to the theoretical capacity of the composite electrode.

tions at the 50:50 and 98:2 ratio, compared to the Zn(OTf)₂ cells.

As all material-electrolyte combinations exhibit a stable capacity utilization and stable cycling at 5 C charging rate, a long-term evaluation was added to the test protocol, which subjected the cells to cycling at 5 C for at least 500 cycles (Figure 8). Stable cycling was observed for both electrolytes at all utilized monomer ratios. In contrast to the rate-capability experiments, no swelling effects and capacity increasing are observed, most probably since the long-term experiment was performed after extensive CV testing, allowing for sufficient equilibration of the system.

The long-term cycling experiments revealed that all investigated systems are capable of stable cycling for 500 cycles at 5 C. The reached material utilizations are in accordance with the rate tests, which suggest a slightly reduced available capacity compared to 1 C cycling. After 500 cycles, the batteries retain over 99% of their initial capacities. The hydrophilicity mediator does not appear to influence the cycling stability or to degrade significantly. The resultant capacity retentions are summarized in Table 2.

The obtained stability of the aqueous system is underlined by float test experiments (Figure 9). Float testing is known from

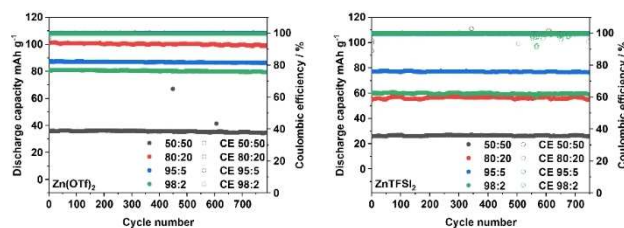


Figure 8. Long-term cycling experiments at a charging/discharging rate of 5 C for 500 cycles.

Table 2. Capacity retention after 500 consecutive galvanostatic cycles at 5 C.

Electrolyte	Feed ratio TEMPO:METAC			
	50:50 [%]	80:20 [%]	95:5 [%]	98:2 [%]
Zn(OTf) ₂	99.5	99.1	99.3	99.4
ZnTFSI ₂	100	99.8	100	99.5

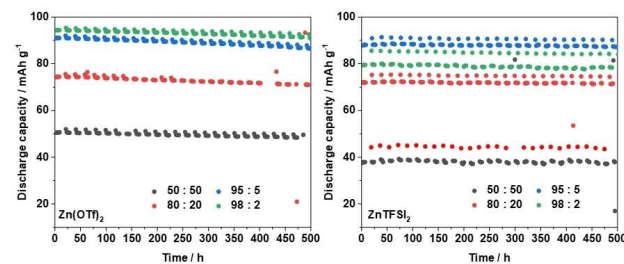


Figure 9. Float test experiments for the Zn(OTf)₂ (left) and ZnTFSI₂ (right) electrolytes. A holding voltage of 1.7 V (vs. Zn/Zn²⁺) was applied for 10 h per repetition, followed by five galvanostatic cycles at 1 C charging rate for a total test duration of 500 h.

the supercapacitor community, where it is used to obtain information about the electrochemical stability of a cell that is kept at high state of charge for extended time periods. In the present case, the batteries were subjected repeatedly to potentiostatic charging for 10 h at 1.7 V with subsequent galvanostatic cycling at 1 C for five cycles. This process is performed for 500 h in total. When the discharge capacities are investigated afterwards, it could be revealed that both $\text{Zn}(\text{OTf})_2$ and ZnTfSI_2 enable a stable floating for 500 h. However, for the ZnTfSI_2 electrolyte, the capacity values vary slightly in the 50:50 ratio system, making it hard to determine the exact capacity loss over time. The strongest decrease of the discharge capacities can be seen for the 95:5 ratio in the $\text{Zn}(\text{OTf})_2$ electrolyte. Here, a pronounced decrease of capacity is observed over the first 200 h of floating. For both electrolytes, the 95:5 ratio leads to the highest overall capacities, despite the fact that 3% less active material is contained in the composite electrodes. At lower hydrophilicity mediator ratios, less active material can be addressed and the material seems less suitable for aqueous electrolytes. Therefore, we consider a mediator ratio of 5% as a kind of “sweet spot” between maintaining the high specific capacity of the pure, hydrophobic PTMA and gaining the hydrophilicity of the poly(TEMPO-co-METAC).

This “sweet spot” is confirmed in self-discharge tests, where the 95:5 ratio composites exhibit the overall lowest self-discharge (Figure 10) with a slightly more pronounced self-discharge of the $\text{Zn}(\text{OTf})_2$ -based cells. As the low self-discharge is observed for the rather hydrophobic polymers, this effect can most probably be assigned to the higher solubility of shorter copolymer chains that show a large percentage of METAC units. Consequent shuttling processes would lead to an iterative discharging of charged TEMPO moieties in the crosslinked polymer network.

Conclusion

In this work, four different 2,2,6,6-tetramethylpiperidiny-*N*-oxyl-co-[2-(methacryloyloxy)-ethyl]trimethyl ammonium chloride (TEMPO-co-METAC) copolymers with monomer ratios of 50:50, 80:20, 95:5, and 98:2 have been synthesized and electrochemi-

cally characterized. Their suitability as active materials in coin cell batteries utilizing aqueous electrolytes was successfully demonstrated. The presented systems revealed good cyclability over at least 500 consecutive cycles at 5 C charging/discharging rate with high capacity retentions greater than 99%. Furthermore, it was shown that only a low amount of solubility mediator (≥ 2 mol%) is sufficient to enhance the hydrophilicity of the active material. This emphasizes the ability of the poly(TEMPO-co-METAC) copolymer to provide the necessary hydrophilicity while maintaining the poly(2,2,6,6-tetramethylpiperidiny-*N*-oxyl-4-methacrylate) (PTMA)-typical battery performance. However, it must be noted that this feature comes at the cost of a pronounced wetting period that is necessary until a maximum number of TEMPO moieties is addressable. To further investigate the material feasibility, self-discharge investigations and float tests have been applied for all material-electrolyte combinations. Here, the best results were obtained for the lowest mediator amount, showing low self-discharge and high capacity retentions after 500 h of floating. All in all, the solubility mediator does not seem to significantly affect the cyclability of the cells. Stable and hydrophilic redox-active polymers were obtained through simple free radical polymerization. This strategy could not only yield new battery materials from materials that have been previously incompatible with aqueous electrolytes but also be of great interest for different application scenarios, where water is the desired electrolyte due to its low-cost, non-toxic and sustainable nature.

Experimental Section

Materials

All materials were purchased from commercial sources. For the syntheses of active materials, 2,2,6,6-tetramethylpiperidiny-*N*-oxyl-methacrylate (TCI), 2-(methacryloyloxy)-ethyl]-trimethyl ammonium chloride (Sigma Aldrich), poly(ethylene glycol) diacrylate (Sigma Aldrich) were used, and inhibitors were removed using an inhibitor remover for hydroquinone and hydroquinone monomethyl ether (Sigma Aldrich). 2,2'-Azobis[2-methylpropionamidin]-dihydrochloride (V-50; Sigma Aldrich) was utilized as received. For the oxidation step, sodium tungstate dihydrate (Acros Organics) and H_2O_2 (50%; ROTH) were used. The utilized zinc-based electrolyte salts ZnTfSI_2 (TCI) and $\text{Zn}(\text{OTf})_2$ (Sigma Aldrich) were used as received.

General synthesis of poly(TEMPMA-co-PEGDA-co-METAC)

The poly(TEMPMA-co-PEGDA-co-METAC) cathode active material was synthesized from commercial materials by radical polymerization (Scheme 2). First, 13.2 mL of water was added to 3 g of TEMPMA (M_n : 225.33 g mol^{-1}) in a microwave vial (20 mL). Then, HCl (37%, 0.7 mL) was added slowly to the suspension. After 5 min of intensive stirring, the pH value was controlled by pH indicator strips (pH 10). Further HCl was added until the TEMPMA was dissolved completely. After every 100 μL of HCl, the pH value was checked to avoid that it decreased below 6. Subsequently, METAC (M_n : 207.7 g mol^{-1}) and PEGDA (M_n : 250 g mol^{-1} ; 2 mol%) as cross-linker were added to the solution according to Table 3. At last, V-50 (2,2'-azobis[2-methylpropionamidin]-dihydrochloride) (M_n : 271 g mol^{-1} ; 4 mol%) as initiator was added and dissolved completely. The vial was sealed and the solution was deoxygenated with argon for

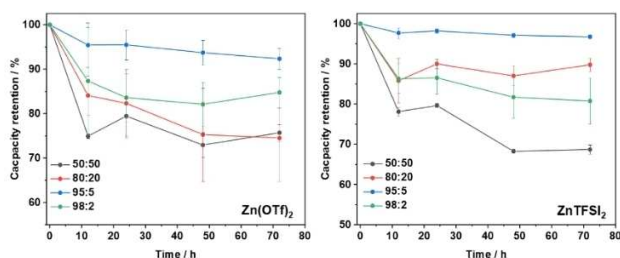
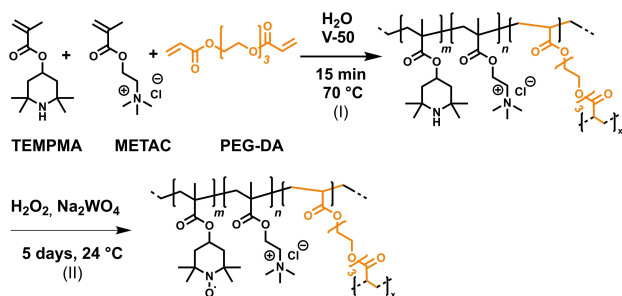


Figure 10. Self-discharge evaluation of the crosslinked copolymers for the $\text{Zn}(\text{OTf})_2$ (left) and ZnTfSI_2 (right) electrolytes. Capacity retention was determined by capacity difference between complete galvanostatic charging at 1 C and galvanostatic discharging after an open-circuit voltage (OCV) period.



Scheme 2. Schematic representation of the general synthesis of poly(TEMPMA-co-PEGDA-co-METAC). (I) Copolymerization and cross-linking; (II) oxidation.

Ratio	Mass TEMPMA [g]	Mass METAC [g]	Mass PEGDA [g]	Mass V-50 [g]
50:50	4.00	3.69	0.18	0.39
80:20	4.00	0.92	0.11	0.25
95:5	4.00	0.19	0.09	0.21
98:2	4.00	0.08	0.09	0.20

30 min. Subsequently, the vial was placed into a pre-heated oil bath (70 °C). After a few minutes, the solution became a solid gel, the vial was removed from the oil bath and opened. After cooling to room temperature, the solid gel was transferred into a round flask (250 mL) and dried overnight by freeze drying. The dry product was ground in a mortar and used directly for oxidation.

General procedure of oxidation

To 1 g of poly(TEMPMA-co-PEGDA-co-METAC), a mixture of water/ethanol (5.3 mL/10.6 mL) was added at 0 °C (ice bath). After 15 min, the suspension was too viscous to be stirred. Thus, a water/ethanol mixture (v:v=1:2) was added until the mixture could be stirred again. Then, Na₂WO₄ (2.6 mol%) and H₂O₂ (50%, 3 eq.) were added to the suspension and the ice bath was removed. All ingredients were added according to Table 4. After 5 min of intensive stirring, the pH value was checked by pH indicator strips (pH 5). Afterwards, NaOH solution (10%) was added until the pH value was between 8 and 10 and the reaction mixture was stirred further. The pH value was checked two times per day and, if necessary, NaOH solution was added. After five days, the oxidation was stopped. The product was separated by centrifugation at 6000 rpm for 10 min. The separated product was isolated and washed with distilled water (3×250 mL). The product was dried overnight in a drying oven (40 °C). The oxidation degree was measured by EPR (electron paramagnetic resonance). X-band EPR spectra were acquired on an EMXmicro CW-EPR spectrometer from Bruker, Germany. The SpinCountQ software module was used for the determination of the spin count. A known PTMA polymer (radical content of 80%, determined through redox titration) was used as a reference. The radical contents of the TEMPO-containing compounds were determined from the mean values derived from the EPR spectra of three individual samples per compound.^[24]

Table 4. Mass loadings of the oxidation and re-oxidation of the copolymers.

Ratio		50:50	80:20	95:5	98:2
First oxidation	Batch size [g]	8.96	7.60	6.70	6.00
	Na ₂ WO ₄ [g]	0.171	0.232	0.242	0.224
	H ₂ O ₂ [mL]	2.03	3.75	3.9	3.7
	Water/ethanol [mL]	125/250	105/210	100/200	120/240
	EPR [%] ^[b]	6.8 ± 2.3	16.0 ± 1.5	55.2 ± 5.4	24.5 ± 2.6
	Ratio		50:50	80:20	95:5
Re-oxidation	Batch size [g]	2.00	2.00	2.00	2.00
	Na ₂ WO ₄ [g]	0.04	0.07	0.08	0.17
	H ₂ O ₂ [mL]	2.50	2.50	2.50	3.50
	Water/ethanol [mL]	30/60	40/80	30/60	60/120
	EPR [%] ^[b]	70.1 ± 2.4	75.1 ± 4.3	73.2 ± 4.4	75 ± 11

[a] Batch was oxidized three times until a sufficient degree of oxidation was obtained. [b] Standard deviation is given from the measurement of three individual samples.

Preparation of TEMPMA-co-PEGDA-co-METAC cathode

The dry synthesized oxidized polymers (750 mg per ball milling process) were ground utilizing a cloud milling method in a ZentriMix 380R (Hettich) at 1500 rpm for 90 min with 1 mm ZrO₂ balls (1 g for each batch). The polymer particles after milling are shown in the Supporting Information (Figure S1). The resultant polymers (500 mg each) were suspended in 7 mL of *N*-methylpyrrolidone (NMP) and PVDF (42 mg) and SuperP® (292 mg) were added. The mixtures were stirred and left overnight to swell at RT. The electrode slurries were subsequently homogenized with a DISPERMAT® at 4000 rpm for 1 h. To optimize the viscosity of the electrode paste, NMP was added during the mixing process (1.5 mL for 50:50 mixture, 3.5 mL for 80:20 mixture, 6 mL for 95:5 mixture and 6 mL for the 98:2 mixture). The homogenized slurries were then drop casted on preweighed graphite disks (Ø 15 mm) as current collectors. The fresh electrodes were then dried in the oven at 80 °C overnight. The theoretical capacities could then be obtained by weighing the electrode discs.

Preparation of coin cells

During the assembly of coin cells (type 2032), the following components were used: two parts of the housing, two spacers and a spring (stainless steel). The cathode part was the dried graphite disk with drop-casted slurry (Ø15 mm). The anode part was a zinc foil (Ø15 mm), without any special preparations. Located between the two electrodes was a glass microfiber separator (Ø19 mm, Whatman™, (GF/D)) with Zn-salt electrolytes like ZnTfSI₂ (2 M) and Zn(OTf)₂ (2 M). The cells were pressed together at an electric crimper machine (MSK-160D) and subjected to electrochemical characterization. The loadings of the electrodes for CV or rate testing analysis were summarized in the subsequent Table 5.

Electrochemical characterization

All electrochemical investigations were performed on a BioLogic BCS-805 potentiostat. Cells were left at RT for 12 h prior to battery testing. All testing protocols started with a 5 min OCV period. Then

Table 5. Summary of the electrode loadings for the CV or rate testing analysis with both supporting electrolyte salts.

Feed ratio	Electrolyte salt	Technique	Loading [mg cm ⁻²]
50:50	ZnOTf ₂	CV	2.33 ± 0.21
		Rates	0.98 ± 0.27
	ZnTFSI ₂	CV	2.11 ± 0.13
		Rates	1.30 ± 0.41
80:20	ZnOTf ₂	CV	2.56 ± 0.11
		Rates	1.79 ± 0.15
	ZnTFSI ₂	CV	1.82 ± 0.55
		Rates	1.56 ± 0.07
95:5	ZnOTf ₂	CV	1.01 ± 0.12
		Rates	1.43 ± 0.19
	ZnTFSI ₂	CV	1.30 ± 0.04
		Rates	1.32 ± 0.19
98:2	ZnOTf ₂	CV	1.92 ± 0.23
		Rates	1.92 ± 0.08
	ZnTFSI ₂	CV	1.96 ± 0.20
		Rates	1.75 ± 0.03

potentiostatic electrochemical impedance (PEIS) was measured with an amplitude of 10 mV in the region of 1 mHz to 1 Hz (60 datapoints per decade). Then 10 min of OCV were recorded before cyclic voltammetry was measured with 0.1, 0.2, 0.5 and 1.0 mVs⁻¹ scanning speed between 0 and 1.85 V. Two cycles were recorded before another 10 min of OCV period were applied. After CV testing, self-discharge tests were performed with a 1 C discharge technique prior to the investigations to ensure complete material discharge before the material is charged. The discharge capacities were then obtained from the charging capacity prior to an OCV rest time and the discharge capacity after the OCV rest times. Rest times of 12, 24, 48 and 72 h were utilized. After self-discharge testing, the material was cycled five cycles at 1 C and then at 5 C until battery failure. With analog cells, rate testing was performed galvanostatically after OCV, CV at 1 mVs⁻¹ and PEIS at 0.2, 1, 2, 5, 10, 20 and 50 C for 5 cycles each. The rate testing is followed by float testing, which comprise five cycles of galvanostatic cycling at 1 C, then a 5 min OCV period, then PEIS and finally application of a 1.7 V potential for 10 h. This order is repeated until battery failure.

Acknowledgements

We gratefully acknowledge the financial support of the Thüringer Aufbaubank (TAB, project 2019 FGR 0080). We thank Steffi Stumpf for the measurements of the SEM images. The SEM facilities of the Jena Center for Soft Matter (JCSM) were established with a grant from the German Research Council (DFG). Open Access funding enabled and organized by Projekt DEAL.

Conflict of Interest

The authors declare no conflict of interest.

Data Availability Statement

The data that support the findings of this study are available from the corresponding author upon reasonable request.

Keywords: aqueous electrolyte · hydrophilic polymer · semi-organic battery · TEMPO · zinc battery

- [1] M. Armand, J.-M. Tarascon, *Nature* **2008**, *451*, 652–657.
- [2] K.-H. Choi, D. B. Ahn, S.-Y. Lee, *ACS Energy Lett.* **2018**, *3*, 220–236.
- [3] a) C. Friebe, A. Lex-Balducci, U. S. Schubert, *ChemSusChem* **2019**, *12*, 4093–4115; b) S. Muench, A. Wild, C. Friebe, B. Häupler, T. Janoschka, U. S. Schubert, *Chem. Rev.* **2016**, *116*, 9438–9484.
- [4] J. Huang, Z. Guo, Y. Ma, D. Bin, Y. Wang, Y. Xia, *Small Methods* **2019**, *3*, 1800272.
- [5] a) Y. Shen, B. Liu, X. Liu, J. Liu, J. Ding, C. Zhong, W. Hu, *Energy Storage Mater.* **2021**, *34*, 461–474; b) M. H. Lee, S. J. Kim, D. Chang, J. Kim, S. Moon, K. Oh, K.-Y. Park, W. M. Seong, H. Park, G. Kwon, B. Lee, K. Kang, *Mater. Today* **2019**, *29*, 26–36; c) X. Liu, S.-C. Lee, S. Seifer, R. E. Winans, L. Cheng, Y. Z, T. Li, *Energy Storage Mater.* **2022**, *45*, 696–703.
- [6] a) J. Xu, C. Wang, *J. Electrochem. Soc.* **2022**, *169*, 030530; b) D. Reber, R.-S. Kühnel, C. Battaglia, *ACS Materials Lett.* **2019**, *1*, 44–51.
- [7] a) J. Shin, D. S. Choi, H. J. Lee, Y. Jung, J. W. Choi, *Adv. Energy Mater.* **2019**, *9*, 1900083; b) F. Wang, O. Borodin, T. Gao, X. Fan, W. Sun, F. Han, A. Faraone, J. A. Dura, K. Xu, C. Wang, *Nat. Mater.* **2018**, *17*, 543–549; c) D. Kundu, B. D. Adams, V. Duffort, S. H. Vajargah, L. F. Nazar, *Nat. Energy* **2016**, *1*, 1–8.
- [8] J. Cui, Z. Guo, J. Yi, X. Liu, K. Wu, P. Liang, Q. Li, Y. Liu, Y. Wang, Y. Xia, J. Zhang, *ChemSusChem* **2020**, *13*, 2160–2185.
- [9] Z. Song, H. Zhou, *Energy Environ. Sci.* **2013**, *6*, 2280–2301.
- [10] a) Z. Cai, J. Guo, H. Yang, Y. Xu, *J. Power Sources* **2015**, *279*, 114–122; b) B. Häupler, C. Rössel, A. M. Schwenke, J. Winsberg, D. Schmidt, A. Wild, U. S. Schubert, *NPG Asia Mater.* **2016**, *8*, e283.
- [11] a) Q. Zhao, W. Huang, Z. Luo, L. Liu, Y. Lu, Y. Li, L. Li, J. Hu, H. Ma, J. Chen, *Sci. Adv.* **2018**, *4*, eaao1761; b) Z. Guo, Y. Ma, X. Dong, J. Huang, Y. Wang, Y. Xia, *Angew. Chem. Int. Ed.* **2018**, *57*, 11737–11741; *Angew. Chem.* **2018**, *130*, 11911–11915.
- [12] a) B. J. Bergner, A. Schürmann, K. Peppeler, A. Garsuch, J. Janek, *J. Am. Chem. Soc.* **2014**, *136*, 15054–15064; b) J. Lee, K. Hyun, Y. Kwon, *J. Ind. Eng. Chem.* **2021**, *93*, 383–387.
- [13] K. Oyaizu, T. Suga, K. Yoshimura, H. Nishide, *Macromolecules* **2008**, *41*, 6646–6652.
- [14] a) K. Nakahara, S. Iwasa, M. Satoh, Y. Morioka, J. Iriyama, M. Suguro, E. Hasegawa, *Chem. Phys. Lett.* **2002**, *359*, 351–354; b) T. Ma, A. D. Easley, S. Wang, P. Flouda, J. L. Lutkenhaus, *Cell Rep. Phys. Sci.* **2021**, *2*, 100414.
- [15] a) E. D. R. Lide, *Handbook of Chemistry and Physics*, CRC Press, Boston, **1991**; b) J. Chen, A. Naveed, Y. Nuli, J. Yang, J. Wang, *Energy Storage Mater.* **2020**, *31*, 382–400; c) M. Z. Iqbal, S. Zakar, S. S. Haider, *J. Electroanal. Chem.* **2020**, *858*, 113793.
- [16] K. Koshika, N. Sano, K. Oyaizu, H. Nishide, *Macromol. Chem. Phys.* **2009**, *210*, 1989–1995.
- [17] K. Koshika, N. Chikushi, N. Sano, K. Oyaizu, H. Nishide, *Green Chem.* **2010**, *12*, 1573–1575.
- [18] T. Hagemann, M. Strumpf, E. Schröter, C. Stolze, M. Grube, I. Nischang, M. D. Hager, U. S. Schubert, *Chem. Mater.* **2019**, *31*, 7987–7999.
- [19] K. Hatakeyama-Sato, H. Wakamatsu, R. Katagiri, K. Oyaizu, H. Nishide, *Adv. Mater.* **2018**, *30*, 1800900.
- [20] J. Winsberg, T. Janoschka, S. Morgenstern, T. Hagemann, S. Muench, G. Hauffman, J.-F. Gohy, M. D. Hager, U. S. Schubert, *Adv. Mater.* **2016**, *28*, 2238–2243.
- [21] S. Muench, P. Gerlach, R. Burges, M. Strumpf, S. Hoepfener, A. Wild, A. Lex-Balducci, A. Balducci, J. C. Brendel, U. S. Schubert, *ChemSusChem* **2021**, *14*, 449–455.
- [22] M. Song, H. Tan, D. Chao, H. J. Fan, *Adv. Funct. Mater.* **2018**, *28*, 1802564.
- [23] T. Janoschka, N. Martin, U. Martin, C. Friebe, S. Morgenstern, H. Hiller, M. D. Hager, U. S. Schubert, *Nature* **2015**, *527*, 78–81.
- [24] M. Zhu, Z. Wang, H. Li, Y. Xiong, Z. Liu, Z. Tang, Y. Huang, A. L. Rogach, C. Zhi, *Energy Environ. Sci.* **2018**, *11*, 2414–2422.

Manuscript received: April 27, 2022

Revised manuscript received: June 8, 2022

Accepted manuscript online: June 20, 2022

Version of record online: July 27, 2022